

Re-entry Module for a Shuttle-Derived Vehicle Launch System

J.R. Tewell* and E.S. Ewing†

Martin Marietta Aerospace, New Orleans, Louisiana
and

D.E. Florence‡

General Electric Space Division, Philadelphia, Pennsylvania

A re-entry module for application to a Shuttle-derived vehicle (SDV) launch system is discussed. The SDV utilizes the basic Space Transportation System (STS) elements in an unmanned launch system configuration. The high-cost components (primarily the propulsion and avionics subsystems) are housed in a module configured for re-entry and reuse. The re-entry module characteristics, based on landing impact dispersions and cross-range requirements, are identified. The ballistic configurations are initially assessed and a lifting body configuration selected. The expected re-entry environments are determined and thermal protection materials incorporated into the module design. The mass properties and an inboard profile of the selected module are presented.

Introduction

IN the past, the evolution of space launch vehicles has been motivated by increasing payload weights and volumes and improved economics. Therefore, it is reasonable to assume that the same motivations will govern the development of launch vehicles in the era of the Space Transportation System (STS)—or Shuttle. For example, there is an increasing recognition that, later in this decade, additional investments will be required to support the growth in the volume and weight of the payloads sent into geosynchronous Earth orbit. To satisfy these future requirements, the U.S. space launch program must remain economically attractive in order to continue to support the growing commercial, foreign, and international market. The Shuttle-derived vehicle (SDV) is a potential companion to the ongoing manned launches of the STS that can meet the growing needs of the nation's space program in an extremely cost-effective manner.

Shuttle-Derived Vehicle

Configuration Description

The SDV is an unmanned cargo carrier consisting of a propulsion/avionics (P/A) module and an expendable payload (P/L) module. The cargo carrier is utilized in place of an Orbiter, while the standard external tank (ET) and solid rocket boosters (SRB) are retained.

The payload capability of this launch vehicle is 150,000 lb to low Earth orbit and provides a substantial performance increase when measured against the basic Orbiter performance capability of 65,000 lb. The SDV payload bay is 25 ft in diameter by 90 ft long.

The propulsion and avionics components are housed in a P/A module that is configured for re-entry, recovery, and reuse. The P/A module, 67,000 lb and about 40 ft in length, contains the Orbiter main and secondary propulsion systems, avionics, electrical power, auxiliary power, and thermal con-

trol systems. Re-entry- and recovery-peculiar systems include an aeroshell structure, thermal protection system, parachutes, retrorockets, and landing gear.

Typical Mission Profile

A typical SDV mission profile is depicted in Fig. 1. The nominal SDV mission lasts 24 h and includes recovery of the P/A module.

After liftoff, SRB separation, re-entry, and splashdown occur as currently scheduled for the STS. The cargo carrier shroud is jettisoned at approximately $t + 250$ s. Main engine cutoff occurs at $t + 475$ s and ET separation at $t + 507$ s, while the ET is still suborbital in velocity. The ET ballistically re-enters the Earth's atmosphere, where breakup takes place prior to impact in the ocean.

Payload deployment activities begin at approximately $t + 2$ h. At $t + 22$ h, or sooner, the P/L module is pointed for re-entry by the P/A module and a deorbit burn is initiated. The P/A module then separates and undergoes re-entry maneuvers, while the P/L module enters the atmosphere, where breakup occurs prior to impact in the ocean. After P/A module re-entry, parachutes, solid-propellant retro and sustainer rockets, and extendable landing gear are employed to land the P/A module softly at the selected recovery site.

Potential land recovery sites within the continental United States were assessed and included Edwards Air Force Base (EAFB) and China Lake in California, White Sands, N. Mex., and other low-population density areas primarily in the southwest (Fig. 2). While it is proposed to eventually recover the re-entry module at the launch sites, EAFB was selected for recovery during the early program phases. Since most SDV missions will place the re-entry module in a 28.5 deg inclination, a cross-range capability of about 400 n.mi. is required to reach a landing site at EAFB.

Deorbit Trades

Deboost of the re-entry module from near-Earth circular orbits was investigated. The trends are shown in Fig. 3 and indicate a retro delta- v of at least 250 ft/s is required to deboost the module from a nominal 160 n.mi. orbit to achieve a controlled re-entry.

These deorbit simulations were made using the optimum retro pitch-down angle and associated thrust orientation, which yields the minimum range from deboost to parachute deployment as shown in Fig. 4. This condition is unique in

Presented as Paper 83-1797 at the AIAA Applied Aerodynamics Conference, Danvers, Mass., July 13-15, 1983; submitted Aug. 30, 1983; revision received Sept. 20, 1984. Copyright © American Institute of Aeronautics and Astronautics, Inc., 1983. All rights reserved.

*Manager, Advanced Programs, Michoud Division. Member AIAA.

†Principal Investigator, Vehicles System, Michoud Division. Deceased.

‡Staff Engineer, Aerothermal Performance.

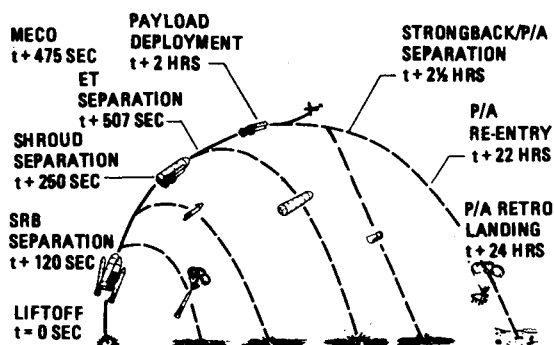


Fig. 1 Typical mission profile.

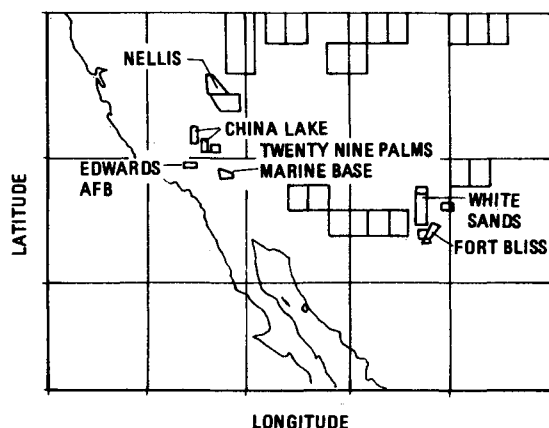


Fig. 2 Potential land recovery sites.

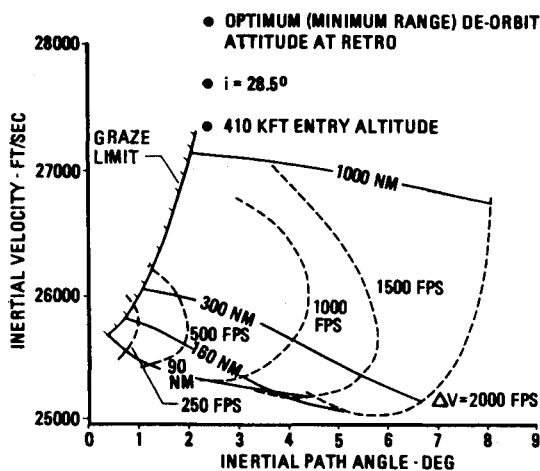


Fig. 3 Inertial re-entry conditions.

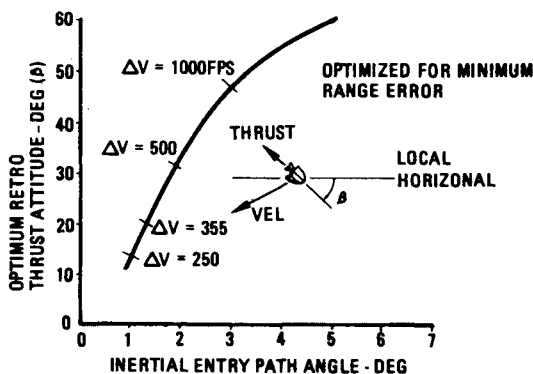


Fig. 4 Deorbit retro attitude.

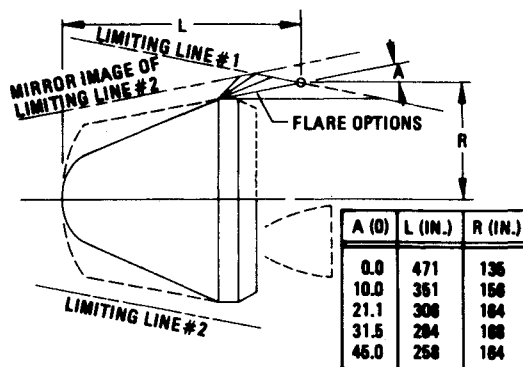


Fig. 5 Ballistic configuration options.

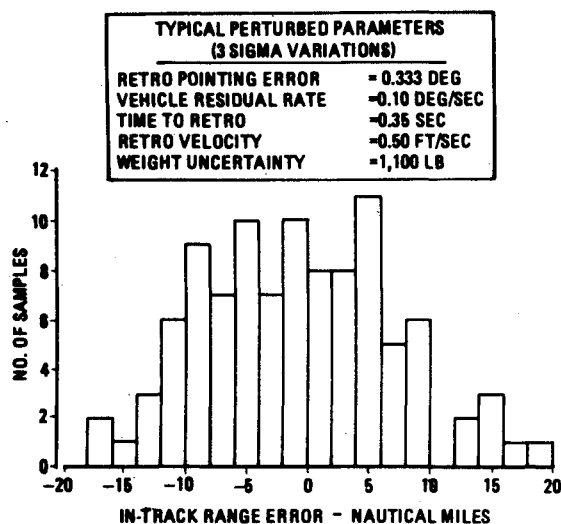


Fig. 6 Impact dispersion.

that errors in the impact location resulting from pitch-down attitude errors are also minimized. For the P/A module, a delta-v of 355 ft/s was selected to assure re-entry from projected orbital altitudes as great as 250 n.mi. The optimum deboost angle was 20 deg, which results in an inertial entry path angle of 1.5 deg.

Ballistic Re-entry System

Configurations

Several ballistic module candidates that met existing SDV configuration envelope constraints were evaluated. The range of possible general configurations varied between the extremes illustrated in Fig. 5. A fairly blunt configuration was selected for the initial evaluations because it met the parachute deployment criterion of a W/C_{DA} less than 180 lb/ft², was statically stable, and experienced reasonably low heat-transfer rates at the stagnation point. Trajectory parameters and entry environments experienced by this configuration were analytically developed.

Impact Dispersion

An assessment of ballistic re-entry impact dispersion was conducted. Degrees of uncertainty associated with the orbital altitude, vector pointing errors, and vehicle rate and weight uncertainties were considered. The results of the Monte Carlo simulations (Fig. 6) indicate that a recovery point error of approximately ± 20 n.mi. may be expected in the ballistic track, while the cross-range error is small at ± 3 n.mi. All but ± 3 n.mi. of the ballistic track error is associated with endoatmospheric flight characteristics. While these errors do not include uncertainties in the parachute performance, this passive

accuracy is sufficient to allow the ballistic re-entry module to impact within the confines of the EAFB perimeter, assuming the orbital ground track passes within the perimeter. However, the majority of SDV launches will occur at inclinations lower than EAFB.

Inclination Change Impacts

The orbit inclination changes required to allow a ballistic re-entry vehicle to reach the EAFB landing site must be achieved propulsively using the onboard orbital maneuvering system (OMS) propellant. In order to quantify just how much propellant is required, three deboost cases were considered: 1) the entire cargo carrier (P/L and P/A modules) is deboosted and provided with adequate inclination change; 2) both the P/L and P/A modules are deorbited, but only the P/A module is provided with an inclination change; and 3) the P/A module is deboosted and given an inclination change, while the P/L module remains on-orbit.

The results are illustrated in Fig. 7 and vividly indicate the propellant weight penalty associated with a ballistic re-entry system if inclination changes are required. A 28.5 deg launch from Kennedy Space Center (KSC) with recovery at EAFB needs an inclination change greater than 6 deg. The preferred approach would be to deorbit both the P/A and P/L module with recovery of only the P/A module; therefore, over 15,000 lb of OMS propellant is required. In summary, it was concluded that attempts to achieve other than minor orbital inclination adjustments—less than 0.5 deg—were very costly weightwise and that the re-entry module cross-range capability must be achieved by the use of a lifting body.

Lifting Body Re-entry System

Lift-to-Drag Requirements

The P/A module lift-to-drag (L/D) requirements were identified for representative SDV launches with return to EAFB. These L/D s for KSC launches are shown in Fig. 8 as a function of orbit inclination and indicate that for single-pass recovery the required L/D range is 2.7-3.5. However, for operational purposes, the maximum P/A module return delay time was baseline at 24 h, which is compatible with SDV turn-

around time requirements. This 24 h on-orbit delay results in the reduction of the required hypersonic L/D to a more workable value of 0.8 (Fig. 9).

Configurations

Numerous lifting asymmetric P/A module configurations were evaluated, all of which accommodated the SDV propulsion and avionics components, while meeting the geometric constraints of avoiding interference with the payload bay and the external tank. The minimum hypersonic L/D goal of 0.8 was not achievable with any of these configurations. Therefore, it seemed prudent to evaluate configurations protruding into the payload bay. Subsequently, the P/L module was stretched to provide an equivalent payload bay length. This permitted the P/A module nose to be lengthened, while using the same forebody geometry. The selected configuration is shown in Fig. 10.

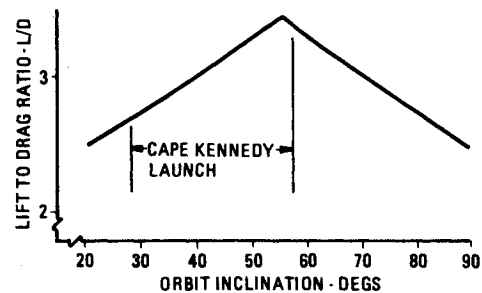


Fig. 8 L/D requirements for single-pass return to EAFB.

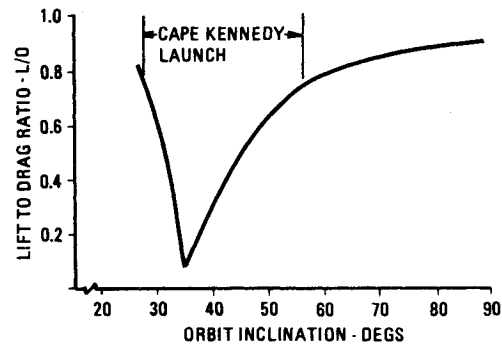


Fig. 9 L/D requirements for one-day return to EAFB.

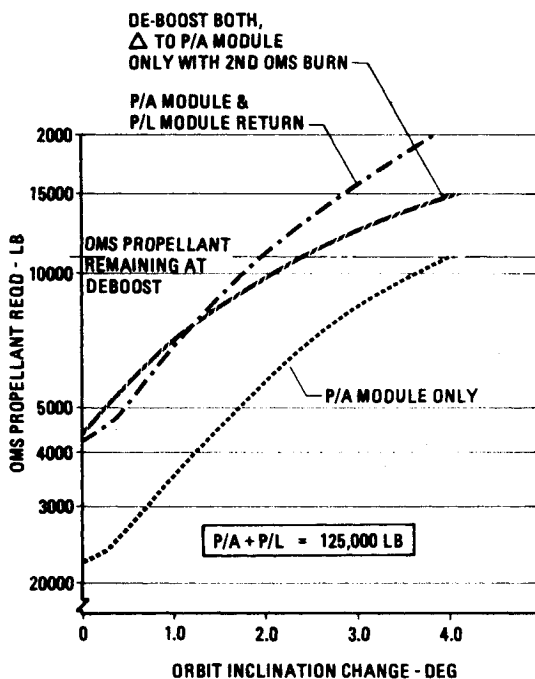


Fig. 7 Re-entry module propellant requirements.

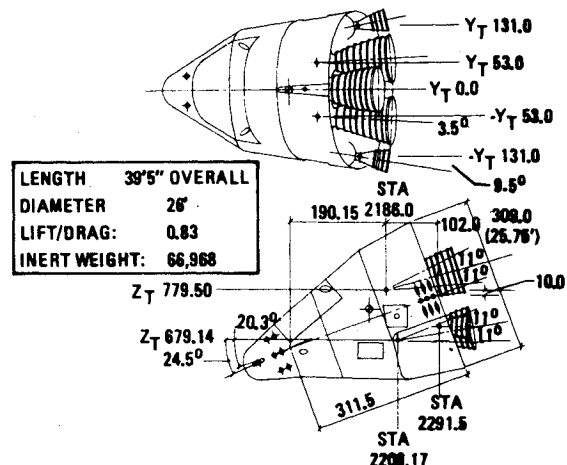


Fig. 10 Biconic lifting body configuration.

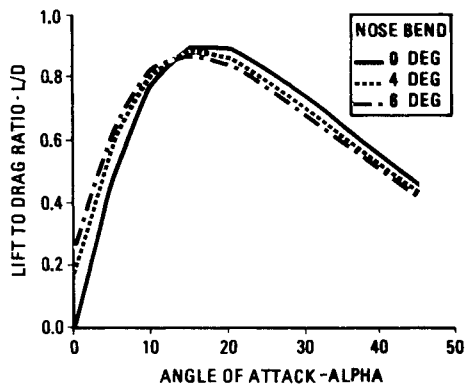


Fig. 11 Effect of nose bend on L/D .

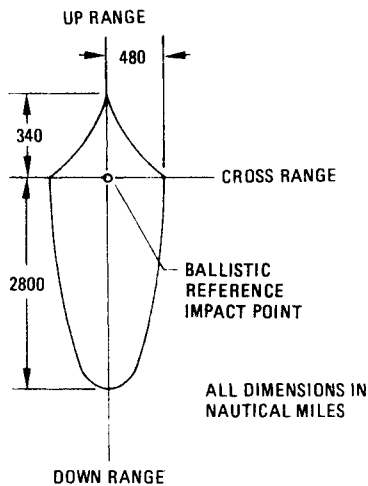


Fig. 12 Lifting body maneuvering capability.

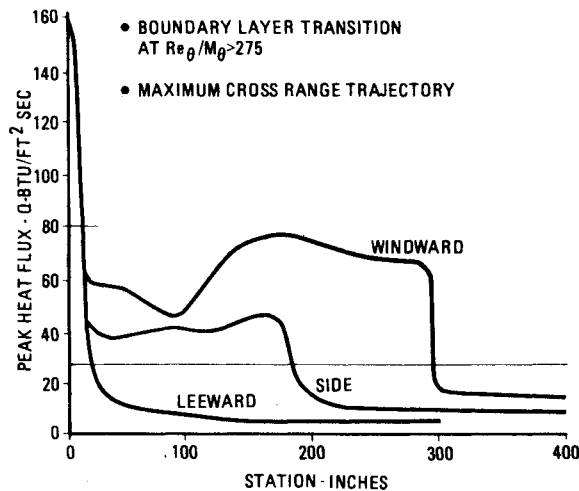
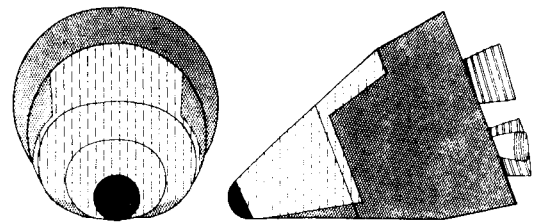


Fig. 13 Peak heat flux distribution.

Hypersonic L/D variation with respect to angle of attack for this configuration is illustrated in Fig. 11 as a function of the nose bend angle. A 4 deg nose bend was selected for the initial aerodynamic evaluations. The hypersonic L/D requirement of at least 0.8 is met with trim angles of attack between 10 and 24 deg. These trim angles are provided with axial center-of-gravity locations $X_{c.g.}/L_{ref}$ of 0.51-0.555.

The sensitivity of the trim angle of attack to the radial c.g. offset was also investigated. For an expected c.g. range of ± 1



ABLATOR MATERIAL	DENSITY LB/FT ³	THERMAL CONDUCTIVITY BTU FT/SQ SEC ⁰ R	SPECIFIC HEAT BTU/LB ⁰ R
■	55	3.10×10^{-5}	0.22
□	25	1.34×10^{-5}	0.30
□	17	0.88×10^{-5}	0.30

REFERENCE PRESSURE - 10^{-1} ATM
REFERENCE TEMPERATURE - 500⁰F

Fig. 14 Thermal protection system.

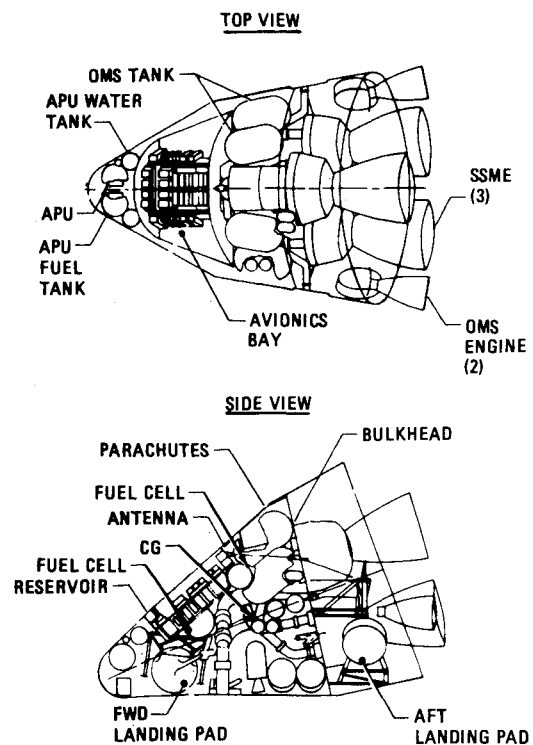


Fig. 15 Re-entry module inboard profile.

in., the trim angle variation is only ± 0.5 deg. The pitch stability for an $X_{c.g.}/L_{ref}$ location of 0.555 is about 7%. Yaw stability, evaluated for a Mach 3 condition, was 5%.

Roll control of the re-entry module is accomplished with the module's reaction control system.

Maneuvering Capability

The maneuvering capability of the selected configuration is shown in Fig. 12. An approximate cross range of 480 n.mi. is possible and a range extension of 2800 n.mi. or range shortening of 340 n.mi. is obtainable with respect to a ballistic impact point. This is more than adequate for landing at EAFB. It should be noted, however, that the actual cross range obtainable depends upon whether the maneuver is made flying west to east or east to west, due to differences in relative

Table 1 Weight summary

Subsystem	Weight, lb
Structure	(16,586)
Thrust structure	3,496
Body (shell)	3,519
TPS	5,295
Internal structure	4,276
Landing and recovery	(6,706)
Parachutes	3,485
Landing gear/legs (4)	3,221
Propulsion	(14,802)
Landing/recovery retrorocket motor	1,320
Helium tanks (MPS)	1,275
OMS subsystem	
Engines (2)	598
Helium tanks (2)	558
Propellant tanks (4)	1,040
Miscellaneous	54
RCS subsystem	(9,957)
Primary thrusters	551
Vernier thrusters	38
Main feed subsystem	4,193
Auxiliary subsystem	4,934
Miscellaneous	241
Power	(3,272)
APU (hydraulic)	1,225
Fuel cells (2)	400
Fuel cells tanks (2)	294
Cabling	428
Black boxes	443
Miscellaneous	482
Avionics	(3,500)
Black boxes	1,425
Antennae (4)	4
Cabling and miscellaneous	2,071
Active thermal control system	(1,126)
P/A module dry weight	(66,968)
P/A module less engines	45,992
Engines (SSMEs, 3)	20,976

velocity and Earth rotation during the time of flight. For entry profiles of long duration, i.e., 15-20 min (which is typical for low Earth orbit, high-lift vehicle entries), the Earth rotation predominates and produces a greater overall larger cross-range capability for maneuvers from east to west.

Thermal Considerations

Hypersonic re-entry heat-transfer analyses were performed for the selected configurations. An axial distribution of the

peak heat flux for the peak heating time is shown in Fig. 13. The maximum heat-transfer rate at the stagnation point is about 160 Btu/ft²·s and, on the forecone windward meridian, a peak turbulent flux of 75 Btu/ft²·s is encountered. On the aft frustum, due to the shallower cone angles, the peak heat-transfer rates reach only 15 Btu/ft²·s. These peak heating rates and heat loads were considered in selecting the re-entry module thermal protection system.

Thermal protection options, using state-of-the-art materials, were assessed. Refurbishable ablative materials were used and the specific areas of material application on the P/A re-entry module are shown in Fig. 14. Note that the nose area experiences heat fluxes high enough to require the use of a high-density elastomeric ablator.

Inboard Profile

An inboard profile and weight statement of the re-entry module are shown in Fig. 15, and Table 1, respectively. Key subsystems identified include the SDV propulsion and avionics, as well as those elements incorporated specifically for recovery and reuse.

Summary

Propulsion/avionics module concepts for application to Shuttle-derived vehicles are feasible and cost effective. While a significant reduction in the re-entry dispersion errors for ballistic re-entry vehicles will be realized during the next decade by the utilization of current state-of-the-art guidance and throttleable liquid/propellant deboost systems, the large propellant weight penalties required to provide inclination changes will prevent their use. Instead, hypersonic lifting bodies will be employed as the practical solution for SDV applications where land recovery is required.

Present state-of-the-art parachute technology impact dispersions will permit recovery of the P/A module at Edwards Air Force Base. However, terminally guided parachute systems for small payloads are already under development where the resulting wind drift errors can be eliminated. This decoupling of the subsonic descent and landing configuration from the hypersonic maneuvering configuration by use of a guided parachute results in a substantially lighter and simpler vehicle than if a compromise vehicle had been designed to handle both flight regimes with a single configuration.

Development during the next decade of terminally guided parachute systems for larger payloads such as the SDV re-entry module, is recommended and will result in the capability to recover the P/A module directly at the SDV launch sites.